

Cyclosporine A Reduces Glial Scarring and Facilitates Functional Recovery Following Transient Focal Ischemia

Hima CS Abeyasinghe², Laita Bokhari^{1,3}, Gregory J Dusting^{4,5} and Carli L Roulston^{1*}

¹Neurotrauma Research team, Department of Medicine, St Vincent's Campus, University of Melbourne, Victoria, Australia

²Department of Surgery, St Vincent's Campus, University of Melbourne, Victoria, Australia

³Department of Biochemistry and Molecular Biology, Bio21 Molecular Science and Biotechnology Institute, University of Melbourne, Victoria, Australia

⁴Cytoprotection Pharmacology Program, Centre for Eye Research, The Royal Eye and Ear Hospital Melbourne, Victoria, Australia.

⁵Department of Ophthalmology, Faculty of Medicine, University of Melbourne, Victoria, Australia

*Corresponding author: Carli L Roulston, Team Leader Neurotrauma Research, Department of Medicine, St Vincent's Campus, University of Melbourne, Level 4, Clinical Sciences Building 29 Regent Street, Fitzroy, Victoria, Australia 3065, Tel: 61 3 9288 3242; Fax: 61 3 9416 2581; E-mail: carlir@unimelb.edu.au

Received date: January 29, 2015; Accepted date: March 27, 2015; Published date: March 31, 2015

Copyright: © 2015 Abeyasinghe HCS et al. This is an open-access article distributed under the terms of the Creative Commons Attribution License, which permits unrestricted use, distribution, and reproduction in any medium, provided the original author and source are credited.

Abstract

Long term survival and success of transplanted stem cells to facilitate recovery from brain injury may involve prolonged use of immunosuppressive agents such as cyclosporine A (CsA). The effect of immunosuppression on overall stroke outcome, in particular endogenous regeneration, is yet to be determined. This study examined the effects of Cyclosporine A (CsA) treatment on brain remodeling events after stroke. Cyclosporine A (10 mg/kg, n=8) or vehicle (2.6% ethanol; 1% castor oil in saline, n=8) was administered prior to endothelin-1-induced middle cerebral artery vasoconstriction in conscious rats, and everyday thereafter for up to 7 days. Treatment with Cyclosporine A significantly attenuated the development of neurological deficits compared to vehicle controls (48hr; $P < 0.05$) but had no effect on infarct volume, activation of microglia/macrophages or critical regenerative responses within the neurogenic niche by 7 days. Treatment with Cyclosporine A did however significantly reduce astrogliosis, in particularly the number of severely diffuse astrocytes present in regions bordering the infarct ($P < 0.05$). Conversely the number of astrocytes ($P < 0.05$) with a pro-survival phenotype were increased with Cyclosporine A treatment. This study suggests that the benefits of Cyclosporine A treatment are not associated with reduced infarct volume but rather retained astrocyte support for preservation of neurotransmission.

Keywords: Focal cerebral ischemia; Immunosuppression; Astrogliosis; Inflammation; Brain rescue; Functional outcome

Introduction

Stroke remains a major cause of death and disability in the industrialized world. Despite attempts to prevent brain injury following ischemic stroke, it is often too late for reperfusion or neuroprotective therapies [1]. Most sufferers end up with long term deficits. For this reason there is a compelling need to develop treatment strategies that promote restoration of functions.

Studies now show that the injured brain is capable of some repair with spontaneous functional recovery observed in a cross section of stroke patients during rehabilitation without pharmaceutical intervention [2]. Subsequently exercise and environmental enrichment strategies have shown some success in improving functional outcomes [3]. To this end, ischemic insults have now been shown to trigger brain remodeling and stem cell migration from the subventricular zone (SVZ) of the lateral ventricle to damaged regions of the brain, even in patients of advanced age [4]. Despite these attempts at repair complete restoration of function is often not achieved [5]. For this reason exogenous cell-based therapy to complement endogenous repair mechanisms are currently being trialed following extensive meta-analysis of over 40 studies reporting significant improvements in function when transplanted after stroke in animal models [6]. Early reports suggest that transplanted embryonic stem cells, fetal stem cells, and immortalized cell lines can survive the grafting process and

improve functional outcome [7,8]. However, the survival and success of transplanting a non-autologous stem cell relies heavily upon preventing host rejection of the graft with immunosuppression routinely used in conjunction with cell-based therapies [9-12].

Cyclosporine A (CsA) is the most widely used immunosuppressive agent in allograft transplant procedures and treatment of autoimmune disorders [13]. Previously, CsA has been shown to be neuroprotective in experimental animal models of stroke [14-16] which has prompted further research into its use as a treatment agent [17]. However, experimental data investigating the effects of CsA in focal models of stroke remain limited with conflicting reports of the efficacy of CsA treatment [16,18-22]. Furthermore, previous preclinical studies have not focused on the effect of CsA on critical cellular events associated with brain repair in response to injury, which is necessary to evaluate the impact of CsA on overall stroke outcome. Using a model of stroke that has been recently characterized and quantified for long term recovery [23] we examined the cellular effects of CsA on microglia activation, astrogliosis, angiogenesis, stem cell proliferation and migration as well as neural differentiation within the neurogenic niche of the subventricular zone (SVZ), 7 days after transient focal cerebral ischemia in rats.

Materials and Methods

The following experiments were conducted in adherence to current RIGOR guidelines [24,25] and included randomization of treatments, blinding during assessment, inclusion of sham and vehicle control

groups, and full statistical analysis involving power calculations in consultation with the Statistical Consulting Centre, University of Melbourne, Victoria, Australia.

Ethics statement

All experiments described were performed in accordance with the guidelines of the National Health & Medical Research Council of Australia Code of Practice for the Care and use of Animals for Experimental Purposes in Australia. The experimental protocol was approved by the St Vincent's Hospital animal ethics committee (AEC009/09). All efforts were made to minimize suffering and ensure animal wellbeing. Paracetamol (2 mg/kg in drinking water) was provided 24 hours prior to and after surgery to minimize distress.

Surgical preparation

Adult male Hooded Wistar rats (300-360 g, n=22, Laboratory Animal Services, University of Adelaide, Australia) were utilized for experiments. All rats were maintained on a 12 hr light/dark cycle at temperatures between 20 and 22 °C, with ad libitum access to food and water. Rats were anaesthetized using a mixture of Ketamine/Xylazine (75 mg/kg; 10 mg/kg respectively i.p.) and maintained throughout surgery by inhalation of isoflurane (95% oxygen and 5% isoflurane). A 23-gauge stainless steel guide cannula was stereotaxically inserted into the cortex 2 mm dorsal to the middle cerebral artery (MCA; 0.2 mm anterior, -5.9 mm lateral, -5.2 mm ventral) as in previous studies [26,27]. Sham control operations (n=3) were performed where animals underwent cannula implantation without stroke to demonstrate that surgery itself does not induce cerebral infarction, as previously described [27]. Rats were allowed to recover for 5 days prior to stroke induction in conscious rats.

Stroke induction

Focal cerebral ischemia was induced in conscious rats by perivascular application of endothelin-1 (ET-1; American Peptide Company, Inc. CA, USA; 60 pmol in 3 µl of saline over 10 min) (n=22) to cause vasoconstriction of the right middle cerebral artery [26]. During endothelin-1 infusion, characteristic behavioral changes were observed indicative of stroke and these responses were graded 1 to 5 according to predictive stroke outcome as in previous studies, with 5 being the most severe [26]. Rats that did not display any behavioral change were deemed not to have suffered a stroke and were excluded from further study. Rectal temperatures were taken with a thermometer probe before stroke and at 30-min or 60-min intervals for 3 hrs after stroke.

Cyclosporine administration

CsA (10 mg/kg, i.p; n=8, Sandimmune, Novartis Pharmaceuticals Corporation, NJ, USA) or vehicle control (2.6% ethanol; 1% castor oil in saline; n=8) was administered 2 days prior to stroke induction and then again everyday thereafter. The dosing regime was chosen based on previous studies demonstrating 10 mg/kg is sufficient to prevent host rejection of stem cell transplants in rats [9]. Pre-treatment of rats with CsA or vehicle did not affect behavioral signs indicative of stroke induction and therefore allowed rats to be assigned a stroke severity score during stroke induction to ensure that within each treatment group stroke severity was equally matched as in previous studies [26].

Assessment of functional outcome

All behavioral assessments were conducted blinded to treatment before any surgical procedures (pre-surgery), immediately prior to ET-1-induced MCA constriction (pre-stroke) and 24, 48, 72 hrs, and 7 days after ET-1-induced vasoconstriction (post-stroke). Animals were evaluated for neurological abnormalities based on detection of abnormal posture and hemiplegia as previously described [28,29]. Asymmetry was evaluated using the adhesive label test by measuring latency to touch and remove attached stimuli from contralateral and ipsilateral forepaws as described previously [29,30]. The neurological function of each rat was compared to pre-stroke scores, such that each rat acted as its own control.

Quantification of ischemic damage

7 days after stroke, rats were decapitated, forebrains removed and frozen over liquid nitrogen, and stored at -80 °C prior to processing. Coronal sections (16 µm thick) were prepared using a Leica cryostat (Leica Microsystems, Wechsler, Germany) at eight pre-determined coronal planes throughout the brain from -3.2 to 6.8 mm relative to Bregma as in previous studies [26,27]. Infarct was determined in triplicate unstained sections using a micro-computer imaging device (MCID M4 image analyzer, Imaging Research Inc., St. Catharines, ON, Canada) according to the methods of Callaway et al. [31] and validated by McCann et al. [32]. Total infarct volume was determined by integrating the cross-sectional area of damage at each stereotaxic level with the distances between levels [33]. The influence of edema was corrected for by applying the following formula: (area of normal hemisphere/area of infarcted hemisphere) x area of infarct [34].

Immunohistochemistry

Immunohistochemical staining was performed in adjacent to identify astrocytes, microglia/macrophages, proliferating SVZ cells, migrating SVZ neuroblasts, radial glial cells, and blood vessels after stroke according to methods described previously [23]. Briefly, tissue sections were fixed in 4% paraformaldehyde (PFA) in 0.1M PBS for 15 min at room temperature, followed by washes then blocked with 5% normal goat serum (NGS) in 0.3% Triton X-100 for 30 mins. Primary antibodies that were diluted in blocking solution included the following: mouse anti-glial fibrillary acidic protein (GFAP; 1:400, Millipore, Billerica, MA, USA), mouse anti-OX42/CD11b (OX42; 1:100, Serotec, Raleigh, NC, USA), rabbit anti-Ki67 (Ki67; 1:1000, Labvision Thermo Scientific, , USA), guinea-pig anti-doublecortin (DCX; 1:3000, Millipore, Billerica, MA, USA), rabbit anti-von Willebrand factor (vWF; 1:200, Millipore, Billerica, MA, USA). Biotinylated secondary antibodies used included goat anti-mouse (1:200, DAKO, Glostrup, Denmark), goat anti-rabbit (1:200, Vector Labs, Burlingame, CA, USA), goat anti-guinea-pig (1:200, Vector Labs, Burlingame, CA, USA), goat anti-rabbit (1:200, Vector Labs, Burlingame, CA, USA). Secondary antibodies were diluted in blocking solution as above. Standard ABC methodology was used to process cells for diaminobenzidine (Sigma, St. Louis, MO, USA) immunohistochemistry and resultant color reaction was visualized with an Olympus microscope (Albertslund, Denmark). Control experiments included either exclusion of each primary antibody from the protocol or the inclusion of the appropriate IgG control to confirm the specificity of each antibody.

Immunofluorescence

Adjacent sections to those used for immunohistochemistry, were used for the detection of cells within the SVZ with dual immunofluorescent techniques as previously described [23]. Briefly, tissue sections were fixed in 4% PFA in 0.1M PBS for 15 min at room temperature, followed by washes then blocked with 5% NGS in 0.3% Triton X-100 for 30 mins. Primary antibodies that were diluted in blocking solution included the following: rabbit anti-Ki67 (Ki67; 1:2000, Labvision Thermo Scientific, USA), mouse anti-GFAP (1:400, Millipore, Billerica, MA, USA), guinea-pig anti-doublecortin (DCX; 1:500, Millipore, Billerica, MA, USA), mouse anti-Nestin (1:400, Cell Signaling Technology, Danvers, MA, USA), and rabbit anti-GFAP (1:400, DAKO, Glostrup, Denmark). Secondary antibodies (1:500 for all) used included; Alexa-568 goat anti-rabbit, Alexa-488 goat anti-mouse, Alexa-488 goat anti-guinea pig. Secondary antibodies were diluted in blocking solution as above. In control experiments, primary antibodies were omitted or the appropriate IgG control was included to verify antibody specificity. Resulting sections were examined with a laser scanning confocal microscope (Nikon Instruments Inc., Melville, NY, USA) using a x40 magnification (a higher magnification was required to achieve greater image resolution for cell counts).

Quantification of immunohistochemistry

Cells of interest were quantified according to our previously published methods [23]. Consistent sample areas for each region were quantified in order to avoid influences of stroke volume on pathological responses (Abeyasinghe et al, 2014[23]). Four common regions of interest where damage was routinely observed were identified in each section for assessment: the damaged cortex, damaged striatum, and the border region surrounding the infarct for both the cortex and striatum. Each analysis area was then compared with the appropriate corresponding mirror region within the contralateral hemisphere (undamaged tissue using the same sample area), as well as to sham-operated controls.

Astrocytes:GFAP labeled reactive astrogliosis was assessed and quantified based on morphological stage of activation [35-37] 7 days post-stroke according to our previous methods [23]. Different gradations of astrocyte transition were identified based on cellular hypertrophy, length and thickness of processes, and categorized as either activated astrocytes or diffuse astrocytes. Activated astrocytes showed some sign of cellular hypertrophy but without significant thickening or overlapping of processes (stellated), whilst diffuse astrocytes displayed a cobblestone morphology with many cells/processes overlapping (indicative of the glial scar) [35]. An automated systematic random sampling point-counting system was applied with a Computer Assisted Stereological Toolbox (CAST System; Olympus) [38]. Quantification of activated or diffuse astrocytes within the cortical and striatal core damage and border regions were counted and expressed as a percentage of the total number of counts (cross hairs) within the defined sample area. The number of resting/quiescent astrocytes was also quantified in the contralateral hemisphere for comparison across treatment groups and to sham-operated controls.

Activated microglia/macrophages: Quantification of OX42 positive cells using the point-counting system were assessed within the same regions of interest as assessed for astrocyte cell counts [23]. OX42 positive cells that displayed activated amoeboid morphology with reduced processes and enlarged cell bodies were counted and expressed as a percentage of the total number of counts (cross hairs)

within the defined sample, and compared across hemispheres, between treatment groups as to sham-operated controls. Resting microglia that displayed morphology with small cell bodies and highly ramified processes were excluded from counts (rarely identified within the damaged zone).

SVZ cell proliferation and neural differentiation:Ki67 positive proliferative cells, proliferating radial glial cells (Ki67/GFAP positive), or migrating immature neurons (DCX positive) within the SVZ were quantified separately at 7 days post-stroke as previously described [23]. Cells within the ipsilateral SVZ and contralateral SVZ were quantified using the cell counter plug-in for National Institute of Health ImageJ software (USA). Ki67 positive images were obtained using an Olympus microscope (Albertslund, Denmark) under x20 magnification, while Ki67/GFAP positive and Ki67/DCX positive images were obtained using a laser scanning confocal microscope (Nikon Instruments Inc., Melville, NY, USA) under x40 magnification. The small counting frame within the SVZ required quantification of cell numbers using standard stereological techniques and ImageJ. The total number of proliferating cells, proliferating radial glial cells, or immature neurons detected in the ipsilateral SVZ was then compared to the corresponding contralateral SVZ and expressed as 100% control. Qualitative images of radial glial cells (Nestin/GFAP positive) observed migrating from the SVZ toward penumbral regions was obtained using a confocal microscope (Nikon) under x40 magnification.

Blood vessels: Blood vessel quantification was assessed 7 days post-stroke in vWF-labeled sections within the same brain regions of interest used for quantification of inflammatory cells using the CAST point-counting system [23]. The number of both small and large vWF labeled blood vessels detected in the ipsilateral sample region was then compared to the contralateral region and expressed as 100% control.

Statistical analyses

Neurological outcome data was analysed by Kruskal-Wallis non-parametric ANOVA followed by Dunn's post-test and deficits were considered improved by a score of 1 with a SD of 1.98. Forelimb asymmetry data were analysed by repeated measures two-way ANOVA (side x hr/days after stroke) to compare latencies in the ipsilateral and contralateral forepaws over time. Infarct area at each stereotaxic position from bregma was analyzed by two-way ANOVA between treatment groups, and infarct volume was analysed using paired t-tests. *Bonferroni post-hoc tests were used to compare between groups, if P<0.05.* Cell counts were analysed by one-way ANOVA followed by *Bonferroni* post-test for comparisons between all groups including shams. Values are presented as mean \pm SEM. To test for correlation between infarct volume and either: inflammatory cell activation, SVZ cell proliferation, migrating SVZ neuroblasts, or angiogenesis the Pearson product-moment coefficient, r , for ordinal values was determined using GraphPad Prism, version 6 (GraphPad Software Inc., San Diego CA). A value of $P<0.05$ was considered significant.

Results

Functional outcome

A total of 19 rats were included in our analysis. Rats that were excluded from this study included two that did not show signs of

having a stroke during ET-1 infusion and one that died as a result of a severe stroke.

ET-1 induced stroke resulted in significant neurological deficits in vehicle treated animals at 24 ($P<0.01$), 48 ($P<0.001$), 72 hrs ($P<0.001$) and 7 days ($P<0.05$, $n=8$, Kruskal-Wallis ANOVA followed by Dunn's post-test; Figure 1A) post-stroke when compared to pre-stroke scores. Rats receiving CsA also displayed deficits from 24hrs to 7 days post-stroke ($P<0.05$, $n=8$, ANOVA; Figure 1A) when compared to pre-stroke ratings. These deficits however were significantly less by 48 hrs in comparison to vehicle treated controls ($P<0.05$, ANOVA; Figure 1A). Given the large difference in means at 48 hr, the precision of the estimates was adequate (95% CI 3.85–6.65 Vehicle; 1.09–4.40 CsA treatment) to establish the presence of a treatment effect.

Latency to touch and remove adhesive labels from the stroke affected contralateral forepaw were significantly increased when compared with the ipsilateral forelimb at 24 (vehicle: $P<0.0001$, CsA: $P<0.001$), 48 (vehicle: $P<0.0001$, CsA: $P<0.05$), and 72 hrs (vehicle: $P<0.01$, CsA: $P<0.05$, Two-way ANOVA) after stroke, but not after this time (Figures 1B-E) No significant differences existed in latency to touch or remove adhesive labels between vehicle and CsA treated rats at any time. Sham-operated animals showed no evidence of neurological deficits displayed after cannula-implant surgery.

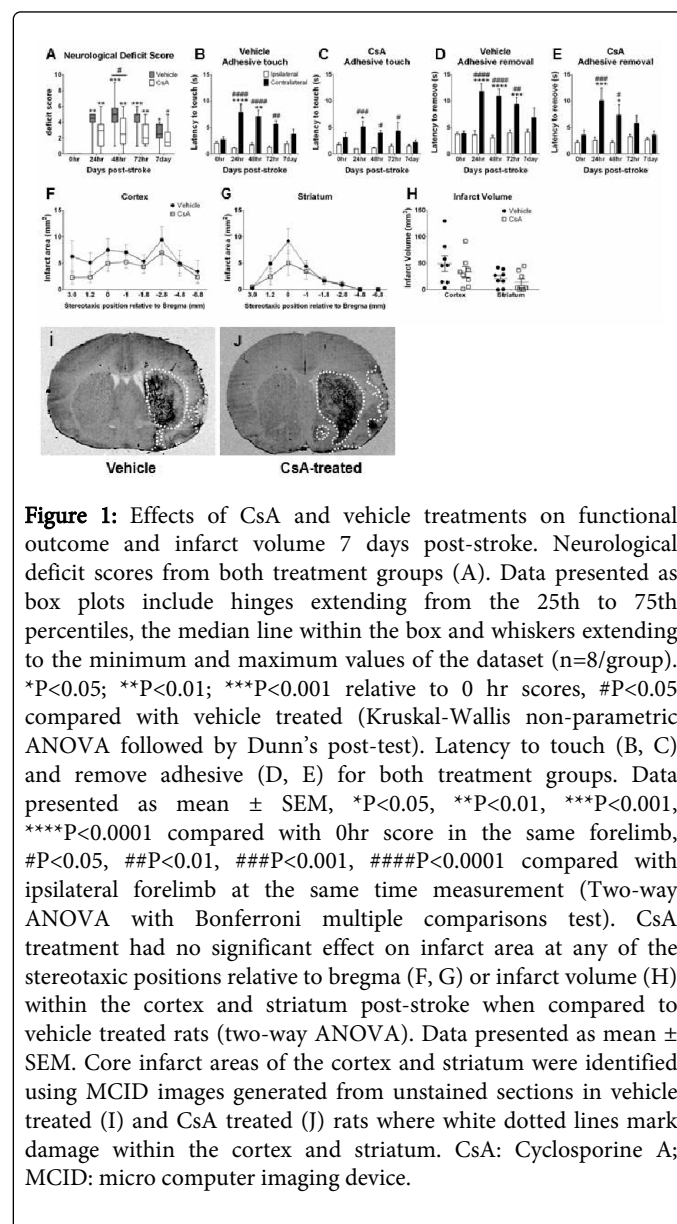
Infarct outcome

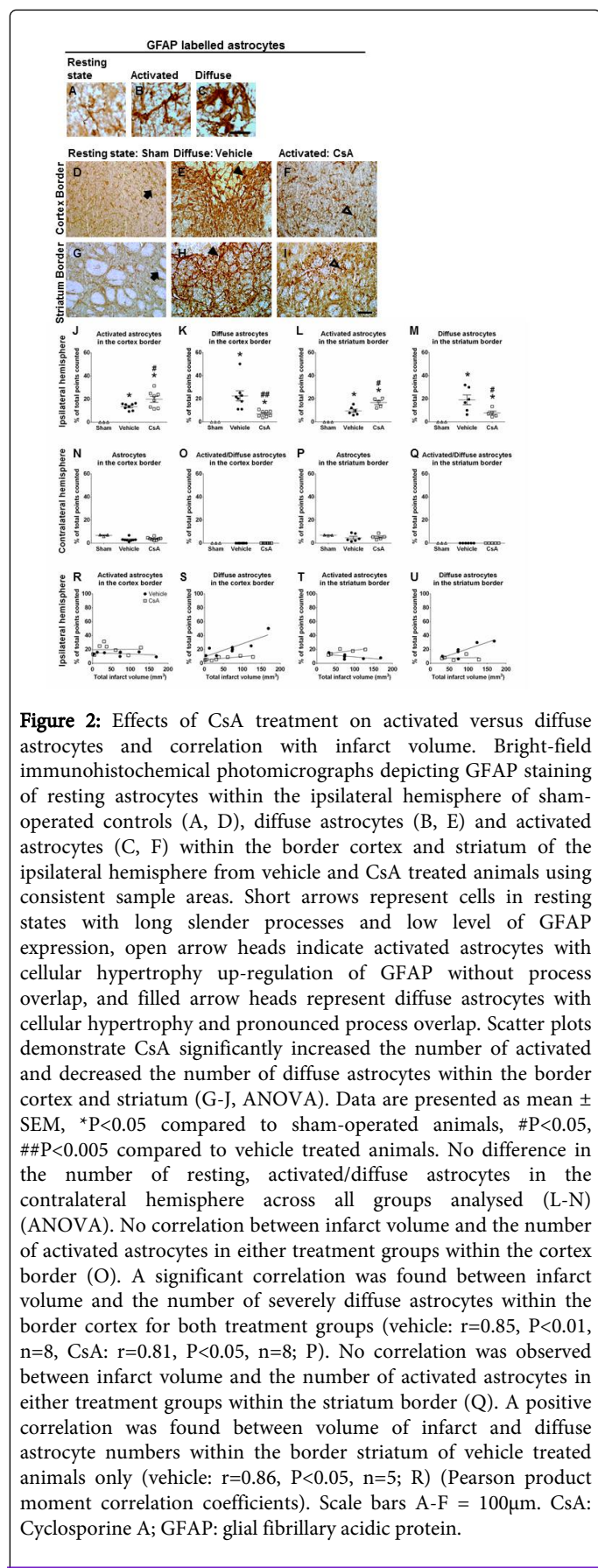
Histological analysis 7 days post-stroke from both treatment groups revealed damage in the parietal, insular, and frontal cortex, and the striatum consistent with previous studies [23,26, 27,39] (Figures 1I, J). Treatment with CsA had no significant effect on infarct area at any anatomical level relative to bregma (Figures 1F, G) or overall volume of infarct (Figure 1H) in the cortex and striatum when compared to vehicle treated control rats. Sham-operated animals showed no evidence of quantifiable ischemic damage in the region of the MCA and were therefore not included in infarct correlation analysis.

Histopathology outcome

Astrogliosis: Astrogliosis was assessed by quantifying astrocytes based on three morphological distinctions. First, astrocytes of normal quiescent appearance were identified by low GFAP expression with long slender processes that did not overlap and were normally found in both hemispheres of sham-operated controls (Figures 2A and 2D) or within regions remote to the infarct site or the contralateral hemisphere of treated animals. Second, severely diffuse astrocytes were identified based on pronounced up-regulation of GFAP expression, hypertrophy of the cell body and processes with distinct process overlap, and dense packing of cells as seen in vehicle treated controls (Figures 2B and 2E). Third, activated astrocytes were defined by an up-regulation of GFAP expression with cellular hypertrophy without pronounced overlap of processes as observed in CsA treated animals (Figures 2C and 2F). Activated and diffuse astrocytes were counted and compared to sham control rats. No astrocytes were present within core infarcted regions analysed and as such only cell counts within the border cortical and striatal regions were presented. The number of activated and diffuse astrocytes within the ipsilateral hemisphere of vehicle and CsA treated rats were significantly greater than sham-operated controls ($P<0.05$ compared to sham-operated animals, scatter plot, ANOVA, Figures 2G-2J). Rats that received CsA treatment showed a significant increase in the number of astrocytes with activated morphologies along with significantly reduced numbers

of astrocytes with severely diffuse morphologies in the surrounding cortical (Activated; $P<0.05$, Diffuse; $P<0.01$, Figures 2G and 2H respectively) and striatal (Activated and Diffuse; $P<0.05$, Figures 2I and 2J respectively) border regions in comparison to vehicle treated animals. The effects of CsA treatment on quiescent resting astrocytes were also examined. Quantification of astrocytes with a resting morphology within the contralateral hemisphere of sham-operated, vehicle and CsA treated animals revealed no significant difference in appearance or number of astrocytes between groups (ANOVA, Figures 2K and 2M). No activated or diffuse astrocytes were observed within the contralateral hemisphere of either treatment group or sham-operated controls (ANOVA, Figures 2L and 2N).



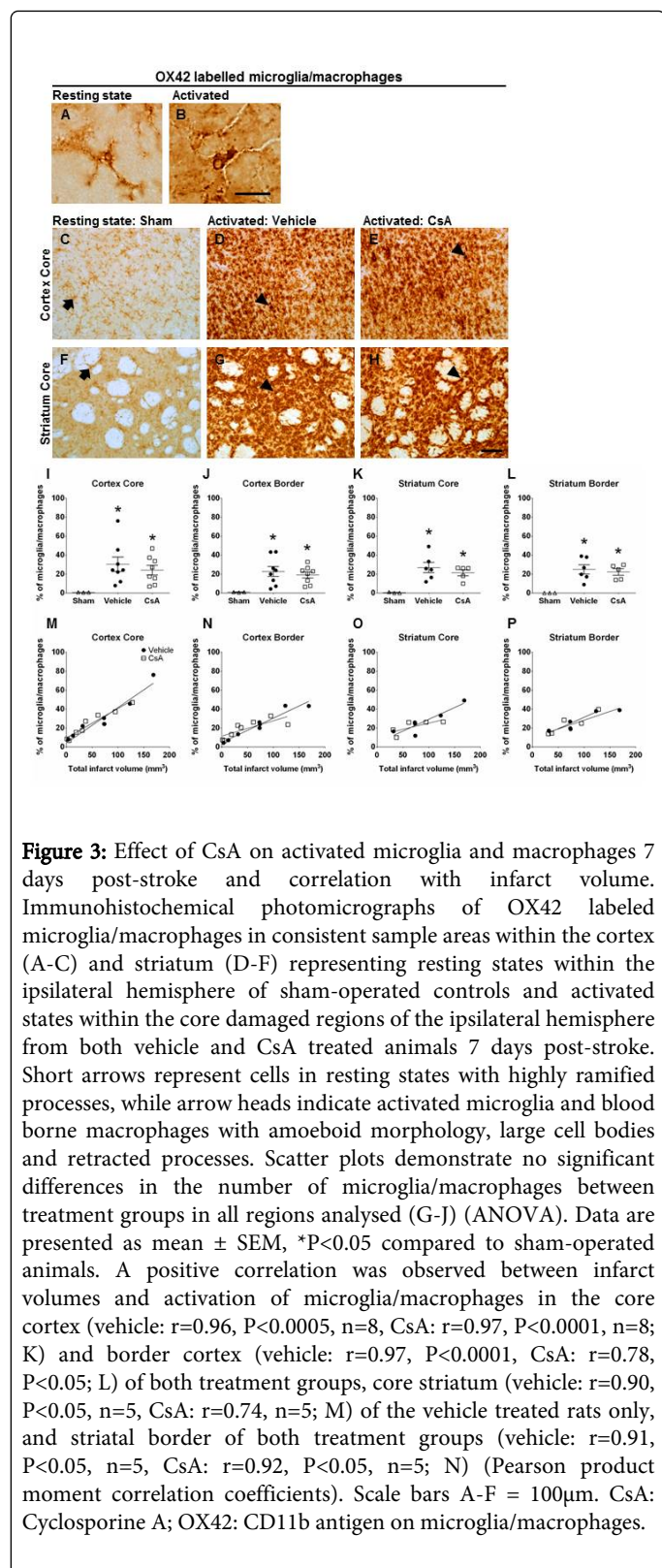


Differences between astrocyte morphological activation across treatment groups was further investigated in relation to stroke severity by comparing the number of activated and diffuse astrocytes across infarct volumes for each treatment group. No significant correlation was observed between activated astrocytes and lesion size in either treatment group within the penumbral regions of the cortex and striatum (Figures 2O, 2Q respectively). In contrast, greater lesion size was found to correlate significantly with a higher number of severely diffuse astrocytes within the border cortex ($r = 0.85$, $P < 0.01$, $n = 8$, Figure 2P) and striatum ($r = 0.86$, $P < 0.05$, Figure 2R) of vehicle treated animals, an effect that was attenuated with CsA treatment despite similar stroke severities.

Microglia/macrophage activation: Microglial/macrophages labeled with OX42 were observed in resting states within the contralateral hemisphere of treated animals or both hemispheres of sham-operated controls, while activated microglia/macrophages were observed in the ipsilateral hemisphere of treated animals. Resting microglia displayed ramified morphology with small cell bodies and long fine branched processes within the ipsilateral cortex and striatum of sham-operated controls (Figures 3A, 3D). Activated microglia appeared amoeboid with large cell bodies and retracted processes similar in appearance to blood derived macrophages. Both activated microglia and blood borne macrophages were quantified together and were mainly observed within the core damaged regions of the cortex (Figures 3B, 3C) and striatum (Figures 3E, 3F) as well as surrounding border areas for both vehicle and CsA treated animals. Following stroke there was a significant increase in the number of activated microglia/macrophages detected across the infarct at 7 days of both treatment groups compared to the ipsilateral hemisphere of sham-operated controls ($P < 0.05$), and was not affected by treatment with CsA compared to vehicle controls (Scatter plots; Figure 3G-3J). Correlation analysis between lesion volume and microglia activation revealed larger infarct volumes correlated with increased numbers of activated microglia/macrophages in both treatment groups in the core cortical (vehicle: $r = 0.96$, $P < 0.0005$, $n = 8$, CsA: $r = 0.97$, $P < 0.0001$, $n = 8$; Figure 3K), cortical border (vehicle: $r = 0.97$, $P < 0.0001$, CsA: $r = 0.78$, $P < 0.05$; Figure 3L), striatal core of the vehicle treated animals only (vehicle: $r = 0.90$, $P < 0.05$, $n = 5$; Figure 3M), and striatal border (vehicle: $r = 0.91$, $P < 0.05$, $n = 5$, CsA: $r = 0.92$, $P < 0.05$, $n = 5$; Figure 3N).

SVZ cell proliferation, migration and neural differentiation: In order to determine the effects of CsA treatment on the neurogenic niche we examined cell proliferation, migration and differentiation within the SVZ (Figures 4A-D). Stroke resulted in an increase in the number of cells positive for Ki67, Ki67/GFAP, and DCX in the ipsilateral SVZ of both CsA treated and vehicle treated rats when compared to the SVZ of the non-ischemic hemisphere, and sham-operated controls (Ki67+ cells and Ki67/GFAP+ cells: $P < 0.05$ for both treatment groups; DCX+ cells: $P < 0.05$, for vehicle treated only, Scatter plots, ANOVA, Figures 4I-K).

Treatment with CsA had no effect on the overall number of Ki67+ proliferating cells, Ki67/GFAP+ proliferating radial glial cells, or the generation of migratory DCX+ neuronal cells within the SVZ when compared to vehicle treated rats (Figures 4I-K).



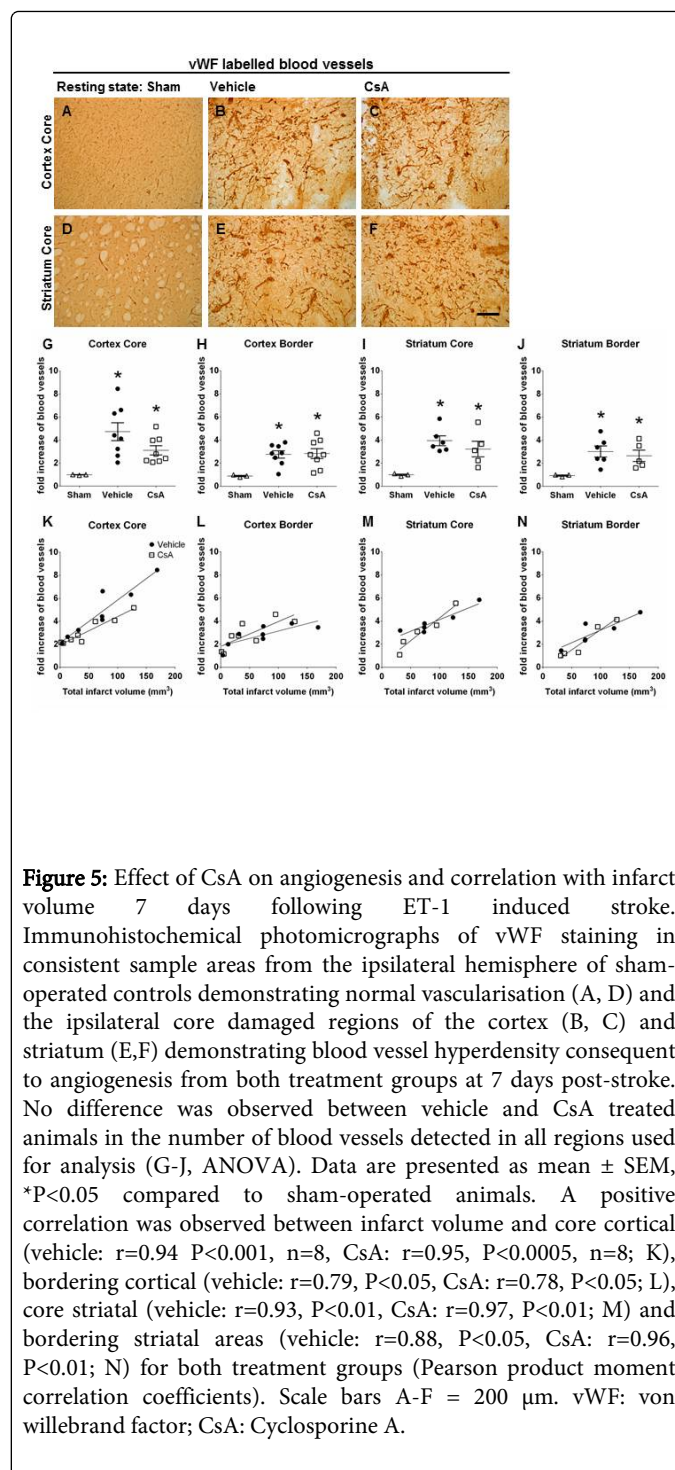
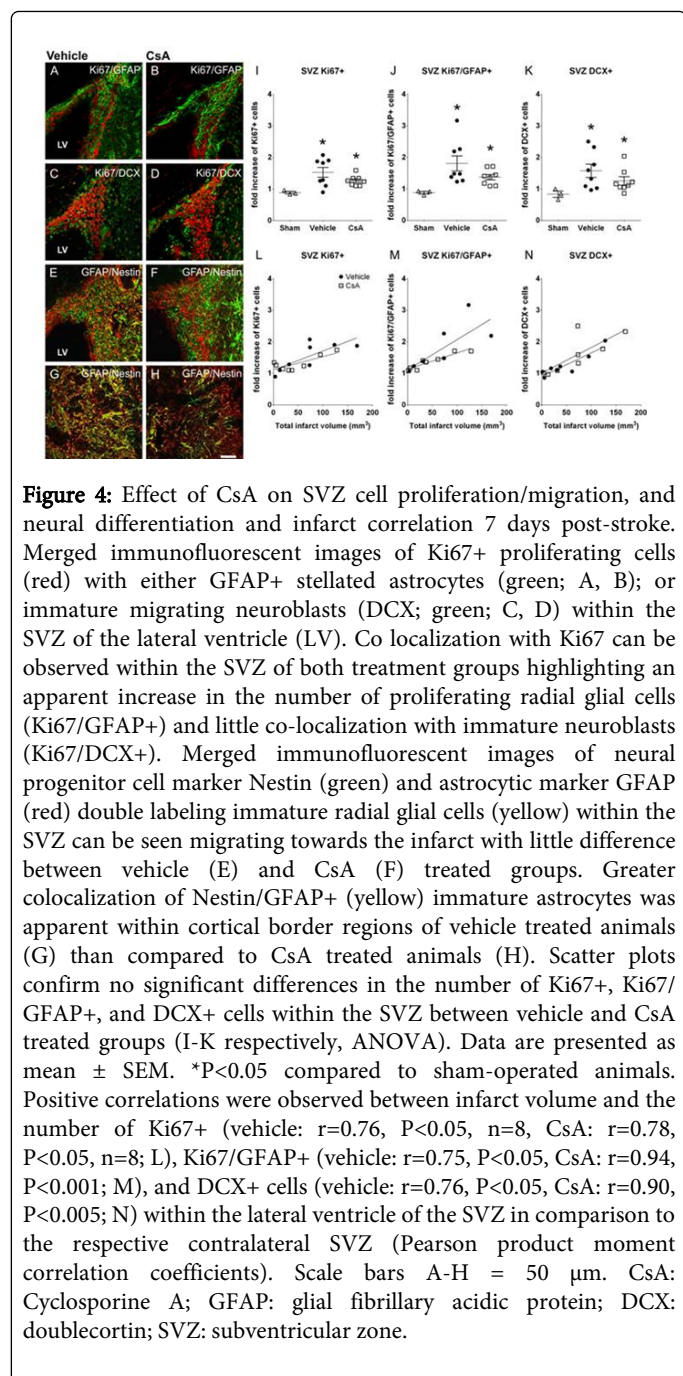
Only GFAP+ astrocytes with stellated phenotypes were quantified within the SVZ as these newly generated astrocytes do not show evidence of being diffuse in morphology.

Comparisons between lesion size and cell numbers within the SVZ revealed larger infarct volumes significantly correlated with an increased number of Ki67+ proliferating cells within the ipsilateral SVZ 7 days from stroke onset for both treatment groups (vehicle: $r = 0.76$, $P < 0.05$, $n = 8$, CsA: $r = 0.78$, $P < 0.05$, $n = 8$; Figure 4L). The same was observed for Ki67/GFAP+ proliferating radial glial cells (vehicle: $r = 0.77$, $P < 0.05$, $n = 8$, CsA: $r = 0.88$, $P < 0.005$, $n = 8$; Figure 4M) for both treatment groups. Similarly, a positive correlation was found between infarct volume and the number of DCX+ immature neuronal cells generated from the SVZ (vehicle: $r = 0.77$, $P < 0.05$, $n = 8$, CsA: $r = 0.91$, $P < 0.005$, $n = 8$; Figure 4N).

Further staining with nestin revealed GFAP+ radial glial cells extending from the SVZ towards injured regions of the brain with no visible differences between treatment groups (Figures 4E and 4F). Although a larger proportion of new Nestin/GFAP+ astrocytes was apparent within the border regions of vehicle treated rats than compared to CsA treated rats (Figures 4G and 4H).

Angiogenesis: vWF immuno-stained blood vessels revealed non-angiogenic regions with organised and disperse blood vessel staining within the contralateral hemisphere of vehicle and CsA treated animals and both hemispheres of sham-operated controls (Figure 5A and 5D). vWF-stained blood vessels also revealed areas of blood vessel hyperdensity consequent of angiogenesis within and around the core cortical (Figures 5B and 5C) and striatal infarcts (Figures 5E and 5F) from both treatment groups. Both large and thin walled microvessels were point counted within a defined sample area (800 μ m²) from the same anatomical region for all rats and compared to the contralateral mirror image for both treatment groups and sham-operated controls. Stroke resulted in a significant increase in angiogenesis in all regions analysed for both treatment groups when compared to the corresponding non-ischemic hemisphere and when compared to sham-operated controls ($P < 0.05$) 7 days post-stroke (Scatter plots; Figures 5G-J). Treatment with CsA had no effect on angiogenesis compared to vehicle treated controls. Blood vessel counts were compared with quantified infarct volume for each rat from both treatment groups. Examination of correlations with ischemic damage revealed a positive correlation existed between the infarct volume and the number of blood vessels in both treatment groups within the core cortex (vehicle: $r = 0.94$ $P < 0.001$, $n = 8$, CsA: $r = 0.96$, $P < 0.0005$, $n = 8$; Figure 5K), border cortex (vehicle: $r = 0.79$, $P < 0.05$, CsA: $r = 0.78$, $P < 0.05$; Figure 5L), core striatum (vehicle: $r = 0.93$, $P < 0.01$, $n = 5$, CsA: $r = 0.97$, $P < 0.01$, $n = 5$; Figure 5M) and border striatum regions (vehicle: $r = 0.88$, $P < 0.05$, CsA: $r = 0.96$, $P < 0.01$; Figure 5N).

Changes in pro-survival astrocytes also corresponded with reduced neurological deficit formation after stroke. Since CsA treatment did not affect infarct size, microglia activation or other brain modelling events, these findings demonstrate a targeted effect on astrocytes for retaining function after stroke.



Functional outcome and infarct volume

Whilst treatment with CsA did not attenuate infarct volume, and functional outcome by 7 days was not significantly different between treatments, it did significantly improve initial neurological deficits post-stroke indicating an early protective effect of CsA on functional loss. Spontaneous recovery often observed even within vehicle control groups is likely to account for a lack of effect between treatment groups by 7 days. None-the-less, CsA treatment did not improve

hemineglect deficits with the adhesive label test at any time after stroke, which highlights the need to incorporate multiple behavioral measures since it is difficult to relate such diffuse damage that results from stroke to a single behavioral measure [40].

Few studies have evaluated pre-treatment of CsA in models of focal ischemia with assessments made 24 hrs-3 days post-stroke [16,21,22,41] and only one study assessed the influence of CsA on functional outcome up to 24 hours with no benefits reported [41]. Behavioural analysis as early as 24 hrs post-stroke may lack sensitivity to detect neurological deficits since maximal infarct volume is not reached until at least 3 days in rodent models [42]. Our study expands on previous data as it is the first to evaluate CsA pre-treatment on both neurological outcome and infarct size beyond 3 days when the infarct has completely matured [27]. It is important to understand that improvements in neurological function after stroke can occur without change to overall stroke volume, as shown with other treatments. Previous studies using Rho-associated kinase (ROCK) inhibitors, Y-27632 and Fasudil, report functional recovery 40 days post-stroke in the absence of neuroprotection [43]. Studies now suggest improved functional outcomes can be achieved without reduction in infarct volume through enhanced plasticity and brain remodeling [43].

Despite the above, studies assessing the effects of CsA on stroke volume in other models of stroke have in contrast reported positive effects when compared to vehicle control animals [44]. These discrepancies may relate to the dose of CsA used. Two high doses of CsA at 20 mg/kg each delivered immediately after reperfusion and 24 hrs post-reperfusion successfully reduced infarct size [45]. However, in the same study a low dose of 10 mg/kg resulted in no change to total infarct volumes and higher doses of CsA ranging from 30-50 mg/kg were associated with high mortality rates, suggesting CsA-induced toxicity. Additionally Cho et al. [41] recently reported reduced infarct volume 24 hours after stroke following pre-stroke treatment with CsA (10 mg/kg), but they did not investigate effects of CsA beyond this recovery time. Yu et al. [19] reported CsA administered at an even lower dose of 1 mg/kg and a second dose of 10 mg/kg demonstrated both non-neuroprotective and neuroprotective effects respectively 3 days post-stroke in a rat model of MCA occlusion. Contrasting data highlights the importance of testing neuroprotective or restorative drug treatments in a variety of experimental stroke models ranging from small to large animals and the incorporation of dose-response studies for appropriate evaluation of preclinical data as outlined by previous STAIR meetings (Stroke Therapy Academic Industry Roundtable) [46].

Effects of CsA on astrocytes

Treatment with CsA significantly reduced the number of diffuse astrocytes known to contribute to extensive glial scar formation surrounding cortical and striatal infarcts [23,35]. Although this is not the first report to show that CsA treatment reduces reactive gliosis after stroke, we now provide quantitative analysis of this effect and distinguish astrocytes based on morphological transition beyond the initial reports conducted up to 48 hours post-stroke [21]. Extending the recovery time is important since astrocytes transition occurs over days to weeks in response to stroke as they dynamically change from supportive to major contributors to glial scar formation [23,27]. By extending recovery to 7 days we show that this transition can be accurately quantified.

Astrocytes are known to exist in a variety of phenotypes that have pro-survival (cytotoxic) and destructive (cytotoxic) components

that arbitrate brain integrity, neuronal death, and subsequent rescue and repair after brain injury [35,36,47,48]. The degree of astrocyte activation is a graded continuum of morphological change that influences brain preservation to long-lasting glial scar formation and is considered manageable by pharmacological intervention [35,49,50]. Strategies aimed at targeting astrocyte activation must be capable of reducing their involvement with glial scarring; however it is equally imperative to retain their pro-survival morphology. Pro-survival astrocytic phenotypes have previously been associated with up-regulation of brain-derived neurotrophic factor (BDNF), glutamate transporters, anti-oxidant enzymes [37] and improved glycogen metabolism [51]. All are vital for restoring neurotransmission. The findings from this study demonstrate that treatment with CsA attenuates the development of neurological deficits possibly through retained astrocyte support (as described by Lau et al. and Sofroniew et al.) [35,36]. Pro-survival astrocytes have previously been shown to be important for neuronal rescue and restoration of neurotransmission, brain plasticity, synaptogenesis and maintenance of the blood brain barrier [35,52].

We previously report that the majority of cells within the neurogenic niche after ET-1 stroke differentiate into astrocytes and extend towards the glial scar, where they are found as diffuse astrocytes incorporated into the glial scar by 14 days [23]. We now report that CsA treatment appears to reduce the transition of radial glial cells into diffuse astrocytes, since many nestin positive astrocytes bordering the infarct retained pro-survival profiles without evidence of overlapping processes typical of cells within the glial scar. We therefore suggest that CsA treatment may also improve the impact of newly generated astrocytes from the SVZ by reducing their contribution to scar formation whilst generating astrocytes for trophic support. Recent reports describe key positive functions of astrogliosis for neuronal support [35,53], thus highlighting the importance of maintaining beneficial effects of reactive astrogliosis with pharmacological strategies.

Initial motor deficits detected after stroke are also due to depression or 'silencing' of surviving pathways and not just the loss of neurons within the core [54, 55]. Spontaneous recovery after stroke is thought to be due to unmasking or activation of these silent pathways with restoration of nerve transmission between surviving cells. This is likely to account for the spontaneous recovery observed in vehicle-treated controls. In this study we have shown the treatment with CsA retains pro-survival astrocyte phenotypes which is important for neuronal support, in particular glutamate re-uptake and ATP availability [35,56,57]. Maintenance of synaptic function by astrocytes is becoming increasingly recognized with astrocytic dysfunction linked to increased synaptic glutamate accumulation and excitotoxicity-mediated neuronal cell death [58-69]. CsA treatment may prevent silencing of pathways within the border regions by permitting glutamate turnover and restoring neurotransmission through retained trophic astrocytic support and thus account for reduced deficits observed by 48 hrs post-stroke. Brunkhorst et al. [67] recently reported functional recovery from stroke following treatment with neuroprotective compound FTY720, a sphingosine-1-phosphate antagonist, with improvements observed attributed to reduced astrogliosis and glial scarring, modulation of synaptic morphology, and increased expression of neurotrophic factors including vascular endothelial growth factor (VEGF) within the border regions of damage. In addition, Taylor et al. [27] previously report that recovery of function after stroke plateaus as scar formation increases within the

border regions of the infarct, indicating an association between glial scarring and functional outcome.

Correlation of treatment with infarct volume

Previous studies report that stroke severity can also affect the degree of pathological response [23,59]. Given this correlation, it was essential to determine if the reduction in astrogliosis after CsA administration was attributed to direct effects of treatment rather than variations in the size of the lesion between treatment groups. An attenuated correlation was observed between diffuse astrocyte numbers and infarct size in CsA treated animals within the cortical border but overall number of diffuse astrocytes was significantly less than that of vehicle treated animals. No correlation was observed between infarct volume and diffuse astrocytic numbers within the striatal border of CsA treated animals. Therefore the increase in the number of activated astrocytes and decrease in the number of diffuse astrocytes in CsA treated groups was directly related to treatment rather than variation in infarct size across groups.

Impact of CsA on microglia/macrophage activation

The brain is thought to be a site that is “immunoprivileged” [60] and reports on effects of CsA on brain inflammation are limited. Microglia are the immune cells of the central nervous system and have been studied in great detail regarding their over activation following injury to the brain [61-63]. Surprisingly we found that CsA had no effect on activated microglia/macrophages 7 days post-stroke suggesting CsA mediated effects appear to be specific to astrocyte transition. This is in direct contrast to recent work where pre-treatment with CsA resulted in reduced microglia/macrophage numbers 24 hours post-stroke [41]. This again highlights the need to incorporate longer recovery periods to enable full maturation of the infarct to occur as well as testing of pharmacological treatments in a variety of stroke models.

Given the initial improvements in functional deficits observed with CsA treatment where changes in microglia responses are not observed, the question arises as to how important is inflammation to stroke outcome [64-66]? The inflammatory contribution from microglia and macrophages following stroke is thought to create a toxic environment that contributes to the spread of damage in the days after a stroke event [39]. Indeed in the present study where CsA has no effect on microglia/macrophage activation we observed no differences in overall infarct in comparison to vehicle control. Any toxic effects on functionally depressed neurons in the penumbra however, may in this case be counteracted due to the positive trophic effects of activated astrocytes, thus resulting in brain rescue. Similar to previous reports, reduced astrogliosis and functional recovery following treatment with neuroprotective compound FTY720 was observed in the absence of attenuation of microglia/macrophages activation [67]. These results suggest that whilst CsA does not affect microglia/macrophage activation, reduction in over-activation of astrocytes and astrogliosis alone may be physiologically beneficial.

CsA effects on SVZ cell proliferation/migration and neural differentiation

When assessing treatments that alter the post-stroke environment it is important to understand the effects on mechanisms associated with neurogenesis. In the present study we demonstrate that treatment with CsA does not alter cell proliferation/migration or neural

differentiation within the SVZ. Normally, the adult SVZ consists of a subpopulation of cells including radial glial cells (type B cells), rapidly dividing transient amplifying cells (type C cells) and migratory neuroblasts (type A cells) [68,69]. In the present study, the total number of Ki67+ proliferating cells, Ki67/GFAP+ proliferating radial glial cells and DCX+ immature migratory neuroblasts generated within the SVZ increased significantly 7 days post-stroke in both treatment groups. CsA administration did not affect overall cell proliferation within the SVZ, identified by Ki67 staining, in comparison to vehicle treated controls. Furthermore, DCX staining, a marker for immature migrating neuroblasts, revealed no significant impairment in neural differentiation within the SVZ following CsA administration relative to vehicle treated control animals.

Stroke increases proliferation and migration of neural progenitor cells within the SVZ towards injured brain regions [70,71], where they have the ability to differentiate into either neurons or astrocytes based on the local microenvironment [69,72,73]. Treatments that aim to improve brain regeneration must therefore avoid negatively influencing this process [23]. In the current study we observed no effect on the number of Ki67/GFAP+ proliferating radial glial cells within the SVZ with CsA treatment. However, in comparison to vehicle treated controls, CsA treatment did appear to reduce the amount of Nestin/GFAP+ staining in the ischemic border zone. This may be due to reduced activation of new astrocytes in this region. Therefore attenuation of astrogliosis with CsA may be due to a collective contribution from reduced differentiation of new progenitor cells into astrocytes, as well as reduced over activation of pre-existing astrocytes. How CsA exerts this effect over astrocyte transition remains to be determined. However the potential of CsA treatment to reduce astrogliosis while releasing trophic factors that support survival and neural differentiation of newly generated progenitor cells is quite promising and represents a desirable treatment outcome.

CsA effect on angiogenesis

Although mature functional blood vessels are not evident until 14 days post-stroke, activated, injured and newly forming blood vessels at 7 days are known to release an array of trophic factors including *VEGF* and brain-derived neurotrophic factor. In addition to being angiogenic, these trophic factors can evoke neurogenesis, are chemotactic for progenitor cells and may enhance the survival and integration of newly generated neuroblasts in the injured brain tissue [3,74,75]. Interestingly VEGF has also been demonstrated to enhance synaptic plasticity [76] and can be beneficial in experimental stroke [77]. Brunkhorst et al. [67] demonstrated up-regulated expression of VEGF within border regions of the infarct following FTY720 treatment associated with reduced astrogliosis, however angiogenesis was not evaluated in their study. In the present study CsA had no effect on the angiogenic response 7 days post-stroke. Combined trophic signaling from angiogenic vessels with reduced astrogliosis may work in concert to support neuronal rescue for functional return.

Conclusion

Pharmacological manipulation of reactive astrogliosis and maintenance of pro-survival astrocytic characteristics has great potential for rescue of neurological deficits that occur due to functional depression in pathways that lay outside of the damaged brain. It has been suggested that reactive astrogliosis and scar formation seen in animal models is reflective of that which occurs in the human brain following stroke [78]. This further highlights the

importance of gaining a better understanding of glial cells and the influence on brain recovery to facilitate the development of therapeutic strategies for future clinical use. Here we provide evidence for the use of CsA for reducing early functional deficits after stroke, even in the absence of neuroprotection. Restorative strategies aimed towards creating a more supportive microenvironment devoid of scar tissue with retained astrocytic support has great potential for early rescue of depressed pathways. Treatments aimed towards overcoming astrogliosis and scar formation could also be used to complement other brain restoration treatments such as cell-based therapies to facilitate their integration and maturation. Given the similarities in glial scar formation between animal models and the human brain after injury, further investigation into novel methods for attenuating astrogliosis may be of great benefit for restoring function in stroke sufferers.

Acknowledgements

This project was financially supported by the National Health and Medical Research Council Australia (NHMRC project grant 628767).

References

1. Donnan GA, Davis SM (2008) Breaking the 3 h barrier for treatment of acute ischaemic stroke. *Lancet Neurol* 7: 981-982.
2. Gauthier LV, Taub E, Perkins C, Ortmann M, Mark VW, et al. (2008) Remodeling the brain: plastic structural brain changes produced by different motor therapies after stroke. *Stroke* 39: 1520-1525.
3. Minger SL, Ekonomou A, Carta EM, Chinoy A, Perry RH, et al. (2007) Endogenous neurogenesis in the human brain following cerebral infarction. *Regen Med* 2: 69-74.
4. Garzón-Muvdi T, Quiñones-Hinojosa A (2009) Neural stem cell niches and homing: recruitment and integration into functional tissues. *ILAR J* 51: 3-23.
5. Muntner P, Garrett E, Klag MJ, Coresh J (2002) Trends in stroke prevalence between 1973 and 1991 in the US population 25 to 74 years of age. *Stroke* 33: 1209-1213.
6. Lees JS, Sena ES, Egan KJ, Antonic A, Koblar SA, et al. (2012) Stem cell-based therapy for experimental stroke: a systematic review and meta-analysis. *Int J Stroke* 7: 582-588.
7. Borlongan CV, Sanberg PR (2002) Neural transplantation in the new millennium. *Cell Transplant* 11: 615-618.
8. Wechsler LR, Kondziolka D (2003) Cell therapy: replacement. *Stroke* 34: 2081-2082.
9. Mukhida K, Mendez I, McLeod M, Kobayashi N, Haughn C, et al. (2007) Spinal GABAergic transplants attenuate mechanical allodynia in a rat model of neuropathic pain. *Stem Cells* 25: 2874-2885.
10. Mukhida K, Hong M, Miles GB, Phillips T, Baghbaderani BA, et al. (2008) A multitarget basal ganglia dopaminergic and GABAergic transplantation strategy enhances behavioural recovery in parkinsonian rats. *Brain* 131: 2106-2126.
11. McLeod MC, Kobayashi NR, Sen A, Baghbaderani BA, Sadi D, et al. (2012) Transplantation of GABAergic Cells Derived from Bioreactor-Expanded Human Neural Precursor Cells Restores Motor and Cognitive Behavioural Deficits in A Rodent Model of Huntington's Disease. *Cell Transplant* 22: 2237-2256.
12. Hicks AU, Lappalainen RS, Narkilahti S, Suuronen R, Corbett D, et al. (2009) Transplantation of human embryonic stem cell-derived neural precursor cells and enriched environment after cortical stroke in rats: cell survival and functional recovery. *Eur J Neurosci* 29: 562-574.
13. Borel JF, Feurer C, Gubler HU, Stahelin H (1976) Biological effects of cyclosporin A: a new antilymphocytic agent. *Agents Actions* 6: 468-475.
14. Uchino H, Elmer E, Uchino K, Li PA, He QP, et al. (1998) Amelioration by cyclosporin A of brain damage in transient forebrain ischemia in the rat. *Brain Res* 812: 216-226.
15. Butcher SP, Henshall DC, Teramura Y, Iwasaki K, Sharkey J (1997) Neuroprotective actions of FK506 in experimental stroke: in vivo evidence against an antiexcitotoxic mechanism. *J Neurosci* 17: 6939-6946.
16. Shiga Y, Onodera H, Matsuo Y, Kogure K (1992) Cyclosporin A protects against ischemia-reperfusion injury in the brain. *Brain Res* 595: 145-148.
17. Osman MM, Lulic D, Glover L, Stahl CE, Lau T, et al. (2011) Cyclosporine-A as a neuroprotective agent against stroke: its translation from laboratory research to clinical application. *Neuropeptides* 45: 359-368.
18. Puka-Sundvall M, Gilland E, Hagberg H (2001) Cerebral hypoxia-ischemia in immature rats: involvement of mitochondrial permeability transition? *Dev Neurosci* 23: 192-197.
19. Yu G, Hess DC, Borlongan CV (2004) Combined cyclosporine-A and methylprednisolone treatment exerts partial and transient neuroprotection against ischemic stroke. *Brain Res* 1018: 32-37.
20. Borlongan CV, Yu G, Matsukawa N, Xu L, Hess DC, et al. (2005) Acute functional effects of cyclosporine-A and methylprednisolone treatment in adult rats exposed to transient ischemic stroke. *Life Sci* 76: 1503-1512.
21. Leger PL, De Paulis D, Branco S, Bonnin P, Couture-Lepetit E, et al. (2011) Evaluation of cyclosporine A in a stroke model in the immature rat brain. *Exp Neurol* 230: 58-66.
22. Kuroda S, Janelidze S, Siesjö BK (1999) The immunosuppressants cyclosporin A and FK506 equally ameliorate brain damage due to 30-min middle cerebral artery occlusion in hyperglycemic rats. *Brain Res* 835: 148-153.
23. Abeyasinghe HC, Bokhari L, Dusing GJ, Roulston CL4 (2014) Brain remodelling following endothelin-1 induced stroke in conscious rats. *PLoS One* 9: e97007.
24. Lapchak PA1 (2013) Recommendations and practices to optimize stroke therapy: developing effective translational research programs. *Stroke* 44: 841-843.
25. Landis SC, Amara SG, Asadullah K, Austin CP, Blumenstein R, et al. (2012) A call for transparent reporting to optimize the predictive value of preclinical research. *Nature* 490: 187-191.
26. Roulston CL, Callaway JK, Jarrott B, Woodman OL, Dusing GJ (2008) Using behaviour to predict stroke severity in conscious rats: post-stroke treatment with 3', 4'-dihydroxyflavonol improves recovery. *Eur J Pharmacol* 584: 100-110.
27. Taylor CJ, Weston RM, Dusing GJ, Roulston CL4 (2013) NADPH oxidase and angiogenesis following endothelin-1 induced stroke in rats: role for nox2 in brain repair. *Brain Sci* 3: 294-317.
28. De Ryck M, Van Reempts J, Borgers M, Wauquier A, Janssen PA (1989) Photochemical stroke model: flunarizine prevents sensorimotor deficits after neocortical infarcts in rats. *Stroke* 20: 1383-1390.
29. Yamamoto M, Tamura A, Kirino T, Shimizu M, Sano K (1988) Behavioral changes after focal cerebral ischemia by left middle cerebral artery occlusion in rats. *Brain Res* 452: 323-328.
30. Callaway JK, Knight MJ, Watkins DJ, Beart PM, Jarrott B (1999) Delayed treatment with AM-36, a novel neuroprotective agent, reduces neuronal damage after endothelin-1-induced middle cerebral artery occlusion in conscious rats. *Stroke* 30: 2704-2712.
31. Callaway JK, Knight MJ, Watkins DJ, Beart PM, Jarrott B, et al. (2000) A novel, rapid, computerized method for quantitation of neuronal damage in a rat model of stroke. *J Neurosci Methods* 102: 53-60.
32. McCann SK, Dusing GJ, Roulston CL3 (2014) Nox2 knockout delays infarct progression and increases vascular recovery through angiogenesis in mice following ischaemic stroke with reperfusion. *PLoS One* 9: e110602.
33. Osborne KA, Shigeno T, Balarsky AM, Ford I, McCulloch J, et al. (1987) Quantitative assessment of early brain damage in a rat model of focal cerebral ischaemia. *J Neurol Neurosurg Psychiatry* 50: 402-410.

34. Leach MJ, Swan JH, Eisenthal D, Dopson M, Nobbs M (1993) BW619C89, a glutamate release inhibitor, protects against focal cerebral ischemic damage. *Stroke* 24: 1063-1067.
35. Sofroniew MV, Vinters HV (2010) Astrocytes: biology and pathology. *Acta Neuropathol* 119: 7-35.
36. Lau CL, Kovacevic M, Tingleff TS, Forsythe JS, Cate HS, et al. (2014) 3D Electrospun scaffolds promote a cytotrophic phenotype of cultured primary astrocytes. *Journal of neurochemistry* 130: 215-226.
37. Lau CL, Perreau VM, Chen MJ, Cate HS, Merlo D, et al. (2012) Transcriptomic profiling of astrocytes treated with the Rho kinase inhibitor Fasudil reveals cytoskeletal and pro-survival responses. *Journal of cellular physiology* 227: 1199-1211.
38. Lokmic Z, Mitchell GM (2011) Visualisation and stereological assessment of blood and lymphatic vessels. *Histol Histopathol* 26: 781-796.
39. McCann SK, Dusting GJ, Roulston CL (2008) Early increase of Nox4 NADPH oxidase and superoxide generation following endothelin-1-induced stroke in conscious rats. *J Neurosci Res* 86: 2524-2534.
40. Windle V, Corbett D (2005) Fluoxetine and recovery of motor function after focal ischemia in rats. *Brain Res* 1044: 25-32.
41. Cho TH, Aguetaz P, Campuzano O, Charriaut-Marlangue C, Riou A, et al. (2013) Pre- and post-treatment with cyclosporine A in a rat model of transient focal cerebral ischaemia with multimodal MRI screening. *Int J Stroke* 8: 669-674.
42. Lansberg MG, O'Brien MW, Tong DC, Moseley ME, Albers GW (2001) Evolution of cerebral infarct volume assessed by diffusion-weighted magnetic resonance imaging. *Arch Neurol* 58: 613-617.
43. Lemmens R, Jaspers T, Robberecht W, Thijs VN (2013) Modifying expression of EphA4 and its downstream targets improves functional recovery after stroke. *Hum Mol Genet* 22: 2214-2220.
44. Matsumoto S, Friberg H, Ferrand-Drake M, Wieloch T (1999) Blockade of the mitochondrial permeability transition pore diminishes infarct size in the rat after transient middle cerebral artery occlusion. *J Cereb Blood Flow Metab* 19: 736-741.
45. Matsumoto S, Isshiki A, Watanabe Y, Wieloch T (2002) Restricted clinical efficacy of cyclosporin A on rat transient middle cerebral artery occlusion. *Life Sci* 72: 591-600.
46. Stair (1999) Stroke Therapy Academic Industry Roundtable Recommendations for standards regarding preclinical neuroprotective and restorative drug development. *Stroke* 30: 2752-2758.
47. McMillian MK, Thai L, Hong JS, O'Callaghan JP, Pennypacker KR (1994) Brain injury in a dish: a model for reactive gliosis. *Trends Neurosci* 17: 138-142.
48. Panickar KS, Norenberg MD (2005) Astrocytes in cerebral ischemic injury: morphological and general considerations. *Glia* 50: 287-298.
49. Ridet JL, Malhotra SK, Privat A, Gage FH (1997) Reactive astrocytes: cellular and molecular cues to biological function. *Trends Neurosci* 20: 570-577.
50. Mueller BK, Mueller R, Schoemaker H (2009) Stimulating neuroregeneration as a therapeutic drug approach for traumatic brain injury. *Br J Pharmacol* 157: 675-685.
51. Hossain MI, Roulston CL, Stapleton DI (2014) Molecular basis of impaired glycogen metabolism during ischemic stroke and hypoxia. *PLoS One* 9: e97570.
52. Gee JR, Keller JN (2005) Astrocytes: regulation of brain homeostasis via apolipoprotein E. *Int J Biochem Cell Biol* 37: 1145-1150.
53. Maragakis NJ, Rothstein JD (2006) Mechanisms of Disease: astrocytes in neurodegenerative disease. *Nat Clin Pract Neurol* 2: 679-689.
54. Font MA, Arboix A, Krupinski J (2010) Angiogenesis, neurogenesis and neuroplasticity in ischemic stroke. *Curr Cardiol Rev* 6: 238-244.
55. Netz J, Lammers T, Hömberg V (1997) Reorganization of motor output in the non-affected hemisphere after stroke. *Brain* 120: 1579-1586.
56. Anderson CM, Swanson RA (2000) Astrocyte glutamate transport: review of properties, regulation, and physiological functions. *Glia* 32: 1-14.
57. O'Shea RD, Lau CL, Farso MC, Diwakarla S, Zagami CJ, et al. (2006) Effects of lipopolysaccharide on glial phenotype and activity of glutamate transporters: evidence for delayed up-regulation and redistribution of GLT-1. *Neurochemistry international* 48: 604-610.
58. Maragakis NJ, Rothstein JD (2004) Glutamate transporters: animal models to neurologic disease. *Neurobiol Dis* 15: 461-473.
59. Nagai N, Kawao N, Okada K, Ishida C, Okumoto K, et al. (2010) Initial brain lesion size affects the extent of subsequent pathophysiological responses. *Brain Res* 1322: 109-117.
60. Mrass P, Weninger W (2006) Immune cell migration as a means to control immune privilege: lessons from the CNS and tumors. *Immunol Rev* 213: 195-212.
61. Nedergaard M, Dirnagl U (2005) Role of glial cells in cerebral ischemia. *Glia* 50: 281-286.
62. Nguyen MD, Julien JP, Rivest S (2002) Innate immunity: the missing link in neuroprotection and neurodegeneration? *Nat Rev Neurosci* 3: 216-227.
63. Wyss-Coray T, Mucke L (2002) Inflammation in neurodegenerative disease--a double-edged sword. *Neuron* 35: 419-432.
64. Iadecola C, Anrather J (2011) The immunology of stroke: from mechanisms to translation. *Nat Med* 17: 796-808.
65. Jin R, Liu L, Zhang S, Nanda A, Li G (2013) Role of inflammation and its mediators in acute ischemic stroke. *J Cardiovasc Transl Res* 6: 834-851.
66. Wang Q, Tang XN, Yenari MA (2007) The inflammatory response in stroke. *J Neuroimmunol* 184: 53-68.
67. Brunkhorst R, Kanaan N, Koch A, Ferreiros N, Mirceska A, et al. (2013) FTY720 treatment in the convalescence period improves functional recovery and reduces reactive astrogliosis in photothrombotic stroke. *PLoS one* 8: e70124.
68. Doetsch F, Caillé I, Lim DA, García-Verdugo JM, Alvarez-Buylla A (1999) Subventricular zone astrocytes are neural stem cells in the adult mammalian brain. *Cell* 97: 703-716.
69. Gregg C, Weiss S (2003) Generation of functional radial glial cells by embryonic and adult forebrain neural stem cells. *J Neurosci* 23: 11587-11601.
70. Zhang RL, Zhang ZG, Chopp M (2005) Neurogenesis in the adult ischemic brain: generation, migration, survival, and restorative therapy. *Neuroscientist* 11: 408-416.
71. Zhang RL, Zhang ZG, Zhang L, Chopp M (2001) Proliferation and differentiation of progenitor cells in the cortex and the subventricular zone in the adult rat after focal cerebral ischemia. *Neuroscience* 105: 33-41.
72. Merkle FT, Tramontin AD, García-Verdugo JM, Alvarez-Buylla A (2004) Radial glia give rise to adult neural stem cells in the subventricular zone. *Proc Natl Acad Sci U S A* 101: 17528-17532.
73. Zhang RL, Zhang ZG, Wang Y, LeTourneau Y, Liu XS, et al. (2007) Stroke induces ependymal cell transformation into radial glia in the subventricular zone of the adult rodent brain. *J Cereb Blood Flow Metab* 27: 1201-1212.
74. Leventhal C, Rafii S, Rafii D, Shahar A, Goldman SA (1999) Endothelial trophic support of neuronal production and recruitment from the adult mammalian subependyma. *Mol Cell Neurosci* 13: 450-464.
75. Shen Q, Goderie SK, Jin L, Karanth N, Sun Y, et al. (2004) Endothelial cells stimulate self-renewal and expand neurogenesis of neural stem cells. *Science* 304: 1338-1340.
76. Licht T, Goshen I, Avital A, Kreisel T, Zubedat S, et al. (2011) Reversible modulations of neuronal plasticity by VEGF. *Proc Natl Acad Sci U S A* 108: 5081-5086.
77. Hermann DM, Zechariah A (2009) Implications of vascular endothelial growth factor for postischemic neurovascular remodeling. *J Cereb Blood Flow Metab* 29: 1620-1643.
78. Huang L, Wu ZB, Zhuge Q, Zheng W, Shao B, et al. (2014) Glial scar formation occurs in the human brain after ischemic stroke. *Int J Med Sci* 11: 344-348.

